DISSOCIATIVE RECOMBINATION OF VIBRATIONALLY COLD CH$_3^+$ AND INTERSTELLAR IMPLICATIONS

R. D. Thomas[1], I. Kashperka[1], E. Vigren[1], W. D. Geppert[1], M. Hamberg[1], M. Larsson[1],
M. af Ugglas[1], V. Zhaunerchyk[1], N. Indriolo[2], K. Yagi[3], S. Hirata[3], and B. J. McCall[4]

[1] Department of Physics, Stockholm University, Albanova University Centre, SE-106 91 Stockholm, Sweden; rdt@fysik.su.se
[2] Department of Physics and Astronomy, Johns Hopkins University, Baltimore, MD 21218, USA
[3] Department of Chemistry, University of Illinois, Urbana, IL 61801, USA
[4] Departments of Chemistry, Astronomy, and Physics, University of Illinois, Urbana, IL 61801, USA

ABSTRACT

CH$_3^+$ is an important molecular ion in the astrochemistry of diffuse clouds, dense clouds, cometary comae, and planetary ionospheres. However, the rate of one of the major destruction mechanisms of CH$_3^+$, dissociative recombination (DR), has long been uncertain, hindering the use of CH$_3^+$ as an astrochemical probe. Here, we present the first absolute measurement of the DR of vibrationally cold CH$_3^+$, which has been made using the heavy storage ring CRYRING in Stockholm, Sweden. From our collision-energy-dependent cross sections, we infer a thermal rate constant of $k(T) = 6.97(\pm0.03) \times 10^{-7}(T/300)^{-0.61(\pm0.01)}$ cm^3 s^{-1} over the region 10 K $\leqslant T \leqslant$ 1000 K. At low collision energies, we have measured the branching fractions of the DR products to be CH$_3$ ($0.00^{+0.01}_{-0.00}$), CH$_2$ + H ($0.35^{+0.01}_{-0.01}$), CH + 2H ($0.20^{+0.02}_{-0.02}$), CH + H$_2$ ($0.10^{+0.01}_{-0.01}$), and C + H$_2$ + H ($0.35^{+0.01}_{-0.02}$), indicating that two or more C–H bonds are broken in 65% of all collisions. We also present vibrational calculations which indicate that the CH$_3^+$ ions in the storage ring were relaxed to the vibrational ground state by spontaneous emission during the storage time. Finally, we discuss the implications of these new measurements for the observation of CH$_3^+$ in regions of the diffuse interstellar medium where CH$^+$ is abundant.

Key words: astrochemistry – ISM: clouds – ISM: molecules – methods: laboratory – molecular processes

1. INTRODUCTION

Dissociative recombination (DR), in which a singly positively charged molecular ion recombines with a free low-energy electron (<1 eV) and subsequently dissociates into neutral fragments, is one of the most important processes driving the chemical and physical evolution of plasmas which are sufficiently cool that they contain molecules, including interstellar clouds, planetary ionospheres, cometary comae, flames, and even the diverter regions of tokamak fusion devices (Salonen et al. 2002).

In many such environments, DR is often the only process that actively reduces the level of ionization in the medium, as it reduces two charged species into neutral particles. The rate at which this reaction occurs together with the products that are formed is of critical importance to the accurate modeling of these environments, and predictions from these models are used to explain experimental and astronomical observations. A recent review article and a book on DR discuss in some detail the importance of this reaction, as well as the tools and techniques used to measure and extract the relevant reaction parameters (Thomas 2008; Larsson & Orel 2008).

CH$_3^+$ is a particularly important polyatomic molecular ion in astrophysical plasmas. It has been measured to be one of the most dominant ions in the innermost coma (<400 km) of comet Halley (Balsiger et al. 1987; Haider et al. 1993; Rubin et al. 2009) and is thought to exist in both diffuse and dense interstellar molecular clouds (Smith 1992), as well as in the Jovian thermosphere at altitudes near and below 400 km (Kim & Fox 1994). In planetary environments, CH$_3^+$ is destroyed either through DR or via ion–molecule/ternary reactions, e.g., in Titan's atmosphere the suggested primary loss is via reaction with methane (Westlake et al. 2012). The DR of CH$_3^+$ is also known to play a major role in interstellar chemistry, especially in diffuse clouds where CH$_2^+$ reacts with H$_2$ to form CH$_3^+$ which

through DR dissociates into CH and CH$_2$ fragments (in dense molecular clouds CH$_3^+$ also undergoes slow radiative association reactions with H$_2$ to form CH$_5^+$; Smith 1992). Astronomical observations of C$_2$ in such clouds had been used to suggest that CH$_2$ should be the main product from the DR of CH$_3^+$ (van Dishoeck & Black 1989), and that a branching fraction of f(CH$_2$) = 0.9 was required; this figure found some support from measurements of the CH$_2$ abundance in Orion-KL and W51M (Hollis et al. 1995). Furthermore, CH$_3^+$ seems to be a useful probe of the physical conditions in the diffuse environment where CH$^+$ is formed; the process(es) leading to high abundance of CH$^+$ remain very poorly understood, and any new diagnostic is of great value. The major uncertainty in the analysis of CH$_3^+$ observations is the DR rate of CH$_3^+$, which in the analysis of Indriolo et al. (2010) was considered to be uncertain by a factor of three either way.

Energy-dependent absolute cross sections for the DR of vibrationally cold CH$_3^+$ ions are therefore of critical importance for better understanding astrophysical environments. Both absolute and relative cross-section measurements of CH$_3^+$ have been previously reported in the literature. However, the only measurements carried out (at the ASTRID storage ring) using vibrationally cool ions were not on an absolute scale (Vejby-Christensen et al. 1997), due to technical difficulties in measuring the weak ion currents in the experiment, and were scaled relative to an earlier set of absolute measurements from a single-pass merged-beam experiment (Mul et al. 1981). In the latter experiment, however, the vibrational distribution of the CH$_3^+$ ions was unknown, but most certainly was not predominantly ground state. Furthermore, there is a subsequently reported factor of two error in their cross-section data (Vejby-Christensen et al. 1997). A subsequent single-pass merged-beam experiment on the DR of the methane family ions that reported absolute cross sections and reaction rate coefficients also had significant
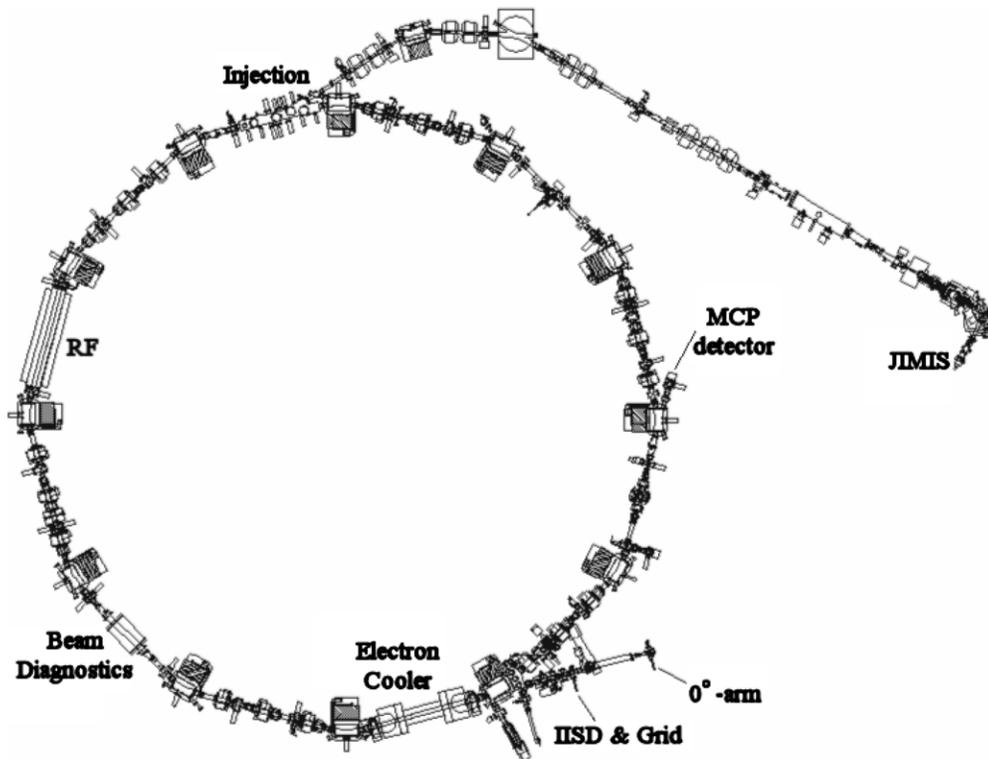
Figure 1. CRYRING ion storage ring. The ions are created in the JIMIS ion source. DR reactions occurring in the electron cooler are measured by the IISD. With these data, both the DR cross sections and, with the grid technique, the branching fractions are determined. The MCP detector is used in combination with the available beam diagnostics to determine the current of the stored ions.

vibrational excitation in the positive ion beam, which necessitated a significant factor of three scaling to extract the ground-state contribution (Sheehan & St.-Maurice 2004).

DR occurs predominantly via two different and competing mechanisms: direct (Bates 1950) and indirect (Bardsley 1968). In the former mechanism, the energy of the incoming electron excites an already bound electron and is captured into a doubly excited neutral state, i.e., onto a deeply repulsive potential surface and the molecule immediately moves rapidly down this surface. In the latter mechanism, the energy of the electron excites the nuclear core and is captured into a rovibronically excited Rydberg state of the neutral molecule which can then couple to the same doubly excited dissociative state that was directly populated in the direct process. In either case, while the energy of the neutral molecule lies above that of the ionic ground state the system can autoionize, although once below this point dissociation is unavoidable (Thomas 2008; Larsson & Orel 2008).

For the collisional-energy-dependent cross sections, a slope of E^{-1} at low collision energies is indicative of a DR process that follows the Wigner threshold law (Wigner 1948), while slopes which differ from this indicate that new and competing reaction channels have opened up: either removing flux from the DR process and transferring it elsewhere, i.e., autoionization, dissociative excitation (DE), dissociative ionization (DI), or increasing the flux into the DR reaction. Deviations from E^{-1} can also manifest themselves in local structures in the cross-section data, i.e., maxima and minima, and studying the behavior of the energy-dependent cross section provides insight into the reaction mechanism and the neutral states involved in the DR process.

A recent theoretical treatment on the DR of CH_3^+ reported by Douguet and co-workers (Douguet et al. 2012;

V. Kokoouline 2012, private communication) has calculated the energy-dependent cross sections from 0 eV to $\approx$0.6 eV. Importantly, they report that at these low collision energies the DR process proceeds exclusively via the indirect mechanism due to the lack of a favorable crossing of any doubly excited neutral state, CH_3^{**}, with the electronic ground state of the ion and, as such, there is zero contribution from the direct mechanism. The vibrational state of the parent CH_3^+ ion should therefore play an important role in the DR reaction and should be especially critical for the relevance of this process in the interstellar medium.

Taken together, no fundamentally reliable data set existed on the DR of this important ion until this work. In the following sections we briefly describe the experimental technique, the data acquisition and analysis, and the storage ring DR results, which include cross sections, thermal rate coefficients, and branching fractions. We then present vibrational calculations that confirm that the CH_3^+ ions in the storage ring relaxed to the vibrational ground state before the DR measurements were made. Finally, we discuss the implications of this work for interpreting CH_3^+ observations in the diffuse interstellar medium.
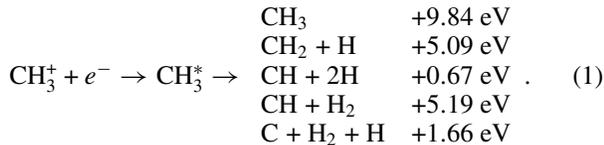
2. EXPERIMENT

The experiment was carried out using the ion storage ring CRYRING, which is located at the Manne Siegbahn Laboratory (MSL), Stockholm University. A schematic view of CRYRING is shown in Figure 1.

This apparatus, the experimental and data acquisition, and analysis techniques, are described in detail in the literature (Thomas 2008; Larsson & Orel 2008) and so only the most essential points are mentioned here. A hollow cathode discharge ion source, JIMIS (Peterson et al. 1998), is used to create the ions of interest using methane as a source gas. The ions were

extracted from the source by a platform potential of 40 kV and injected into the ring. The ions are accelerated further in the ring to a maximum energy of 6.4 MeV by a radio frequency (RF) drift tube. During each revolution the ions pass through the electron cooler region where they interact with a continuously renewed mono-energetic electron beam, whose velocity could be controlled by tuning the cathode voltage of the electron gun in the cooler. Through Coulomb interactions the warm ions transfer heat to the cold electrons and this decreases the phase space occupied by the ions, reducing both their thermal velocity spread and the physical (transverse) size of the ion beam. As a result of this process the resulting transverse temperature distribution of the ion beam approaches that of the electrons, which have a velocity distribution described by an anisotropic Maxwell distribution with $kT_\parallel = 0.1$ meV and $kT_\perp = 2$ meV. The ions are stored in this manner for several seconds in order to achieve vibrational relaxation to the ground state through spontaneous emission. In addition to cooling the ion beam, the electrons also serve as the target for the DR reaction.

In ≈ 0 eV collisions with free electrons, the following are energetically open DR reaction channels assuming that the reaction proceeds via the indirect mechanism:

$$CH_3^+ + e^- \rightarrow CH_3^* \rightarrow \begin{array}{ll} CH_3 & +9.84 \text{ eV} \\ CH_2 + H & +5.09 \text{ eV} \\ CH + 2H & +0.67 \text{ eV} \\ CH + H_2 & +5.19 \text{ eV} \\ C + H_2 + H & +1.66 \text{ eV} \end{array} \quad (1)$$

The energy quoted in each channel is available to the products as kinetic and/or internal energy, where any internal excitation of the fragments reduces the amount available for kinetic energy.

In addition to the neutral products produced from the DR reactions, collisions of the parent ions with residual gas particles also lead to similar neutral fragments, e.g., CH, H, etc. All neutral particles produced in the interaction region are not bent by the dipole magnet located directly after the electron cooler and so tangentially leave the ring down the zero degree arm where they are detected by an ion-implanted silicon detector (IISD). Signals from the IISD detector are recorded either by a multi-channel analyzer (MCA) or a multi-channel scaler (MCS) card located in a PC. Data acquired by the MCA are used to determine the reaction products, i.e., which reaction channels are populated, while data acquired by the MCS are used to determine the energy-dependent cross sections of the DR reaction.

An independent detector, a micro-channel plate detector (MCP), also monitored the neutral particles originating from collisions of the ions with residual gas particles in a straight section just after the electron cooler. These signals are directly proportional to the number of ions in the ring. The pressure in the majority of the storage ring is below standard measurement capabilities, i.e., $< 10^{-11}$ torr, although the cooler region is a little higher and measurable: low $\times 10^{-11}$ torr. In the cooler region, pressure changes of 10% are measurable and variations are kept as low as possible, and the pressure is logged during data acquisition. The effects of short-term pressure bursts, i.e., during a single machine cycle, are averaged out with respect to all the data collected. If such events occur often, this usually points to more serious issues and these are dealt with before the experiments are restarted. Furthermore, to ensure that longer term drifts do not influence the data unduly, e.g., from temperature fluctuations during 24 hr, data are saved every couple of hours.

3. DATA ACQUISITION AND ANALYSIS

Detailed descriptions of the data acquisition and analysis procedures are available in the literature (Thomas 2008; Larsson & Orel 2008) and so are only briefly described here. To allow cooling of the ions, the electrons and ions are held at the same velocity during the first 4.4 s of every ring cycle. For 6.4 MeV ions this corresponds to electrons with an energy of ≈ 234 eV, the "cooling-voltage." After this time the measurements are initiated and the measurement protocol is dependent on whether it is the DR cross sections or product branching data which are to be determined. The former is discussed first.

3.1. DR Cross Sections and Thermal Rate Constants

CH_3^+ is present in such different environments that DR of this ion needs to be investigated over a relatively large range of collision energies. In the present experiments, two regions were investigated: 0–1 eV and 0–20 eV. DR at the lower energies, <1 eV, is of critical importance to the interstellar and ionospheric plasmas, while that at higher energies is relevant to the diverter region of fusion plasmas (for example, the measurements over the region 0–20 eV).

The cathode voltage of the electron cooler is increased to a value corresponding to a center-of-mass collision energy of ≈ 20 eV and where the electrons are faster than the ions. The cathode voltage is held at this value for 100 ms after which, over 2100 ms, it is linearly decreased to a value that also corresponds to a center-of-mass collision energy of ≈ 20 eV but where the electrons are slower than the ions. After 100 ms it is tuned back to the cooling voltage.

The cross sections at high collision energies are significantly smaller than at ≈ 0 eV and become vanishingly smaller (Vejby-Christensen et al. 1997). Non-DR processes such as DE and DI become dominant processes at these and higher collision energies (Bahati et al. 2009). Signals measured at these energies are predominantly from non-DR processes and are fitted using an exponential fit and subtracted from the data to give pure DR counts. To ensure that the correct non-DR background contributions are subtracted from the 0–1 eV measurements these signals can be related to the ion-beam current via the signals measured by the MCP detector.

Measurements of the 0–1 eV region were taken in a similar fashion, and Figures 2(a) and (b) illustrate the relationship between the cathode voltage and the collision energy, respectively, and Figure 2(c) plots example raw IISD-MCS data (triangles) and MCP-MCS data (dots).

The experimental DR collision-energy-dependent rate coefficient, α, can be obtained from

$$\alpha = \frac{dN}{dT} \frac{v_e v_i q^2}{I_e I_i} \frac{\pi r_e^2}{l}, \quad (2)$$

where dN/dT is the number of DR events per unit time, $I_{e,i}$ and $v_{e,i}$ are the currents and lab-frame velocities of the electrons (e) and ions (i), respectively, q is the elementary charge, l is the length of the interaction region ($l = 0.85$ m), and r_e is the radius of the electron beam ($r_e = 2.0$ cm; Danared et al. 2000). The absolute ion current, I_i, was measured at the end of the acceleration phase using a calibrated capacitive pick-up (Paal et al. 2006) and related to the data simultaneously obtained by the MCP detector, defining the proportionality of the ion current to the intensity of the background signals.

Several corrections need to be applied before the data can be fully analyzed. Drag force effects were neglected due
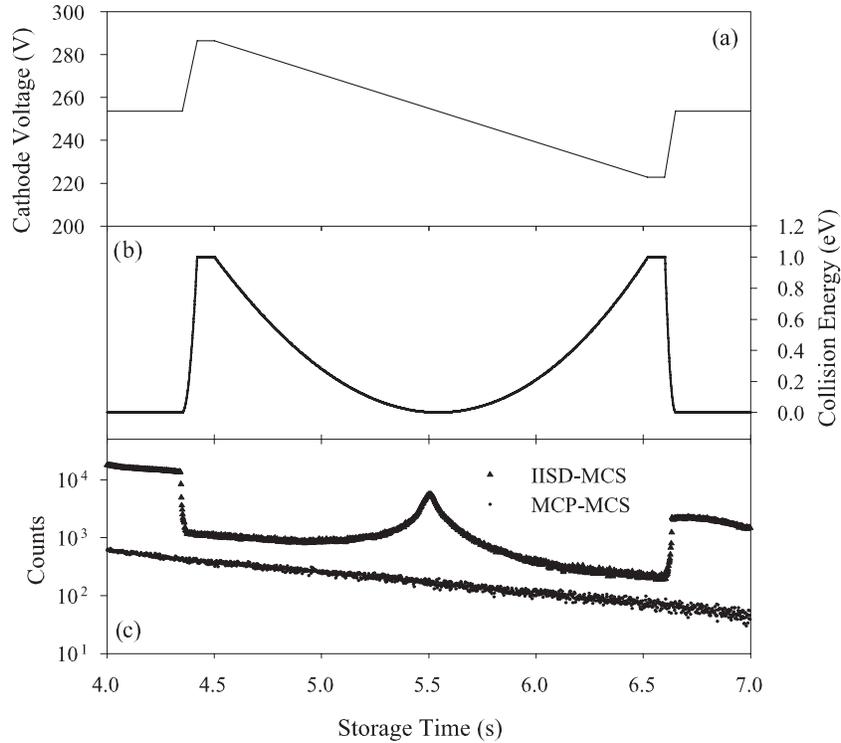
Figure 2. (a) The value of the electron cooler cathode voltage and (b) the corresponding center-of-mass collision energy. (c) The neutral fragments detected by the MCS coupled to the IISD (triangles) and the MCP (dots). All data are plotted as a function of the storage time of the ions in the ring.

to the large mass difference between ions and electrons (Danared et al. 1994). However, the following had to be accounted for: (1) space charge effects in the electron beam, (2) collisions in the regions where the electron beam is bent into and out from the interaction region possess higher relative kinetic energy, and (3) the electrons have a non-negligible velocity spread at low collision energies. Procedures for treating the first two of these contributions are discussed extensively in the literature (DeWitt et al. 1996; Lampert et al. 1996) and so we only comment briefly on the latter.

The energy-dependent DR cross section was extracted from the measured rate coefficient, α, via

$$\alpha = \langle \sigma v_{\rm rel} \rangle = \int v_{\rm rel} f(v_{\rm rel}) \sigma(v_{\rm rel}) d^3 v_{\rm rel}, \qquad (3)$$

where $f(v_{\rm rel})$ is the relative electron velocity distribution. In the current analysis only the electrons' transverse velocity spread was considered, all other velocity spreads being much smaller (Thomas 2008; Larsson & Orel 2008). At large collision energies the energy-dependent DR cross sections, $\sigma(E_{\rm cm})$, are simply obtained by dividing the rate coefficient by the electron center-of-mass velocity, otherwise the cross section is extracted by use of a well-established deconvolution procedure (Mowat et al. 1995).

For astrochemical modeling purposes the DR thermal rate constant, $k(T)$, at low temperatures is a more useful parameter. To determine the thermal rate constant at a specific (electron) temperature the cross section is integrated over the isotropic Maxwellian electron speed distribution that is assumed to be present at that temperature:

$$k(T) = \frac{8\pi m_e}{(2\pi m_e k_B T)^{3/2}} \int_0^\infty E_{\rm cm} \sigma(E_{\rm cm}) e^{-\frac{E_{\rm cm}}{k_B T}} dE_{\rm cm}, \qquad (4)$$

where m_e is the electron mass, k_B is Boltzmann's constant, T is the electron temperature, and $E_{\rm cm}$ is the center-of-mass energy.

Experimental parameters such as $v_{i,e}$ and r_e are known to high precision, while the statistical uncertainties associated with counting particles (dN/dT) are minimized by counting for a sufficiently long time. Uncertainties in the evaluation of the cross sections and thermal rate coefficient are dominated by the uncertainties in measuring $I_{e,i}$ and knowledge of the length of the interaction region, l. Taking these into consideration, the uncertainty quoted in cross-section data reported from CRYRING is $\approx$10%–15% at low collision energies ($<$1.0 eV) and $\approx$15%–20% for higher collision energies, where the usually lower values for the cross sections mean that the statistical uncertainties start to become more significant.

3.2. DR Product Branching

The grid technique was used to determine the population of the open channels given in Equation (1) in which a metal grid with a known transmission factor of $T = 0.297 \pm 0.015$ (Neau et al. 2000) was inserted directly in front of the detector. Individual fragments then have identical probabilities of passing through the grid and being detected and the recorded pulse height spectrum shows a series of peaks that correspond to the total mass of the particles that were not stopped by the grid. A complete data set necessary to fully determine the chemical branching consists of four measurements in which the collision energy is held at either $\approx$0 eV or $\approx$1 eV and the metal grid is either present or removed. During each of these measurements the neutral particle signal monitored by the MCP detector is also recorded—the same detector was used for ion-current normalization. Data taken with the collision energy held at $\approx$1 eV are necessary to account for the background contributions to the measured signals. After background subtraction the pure
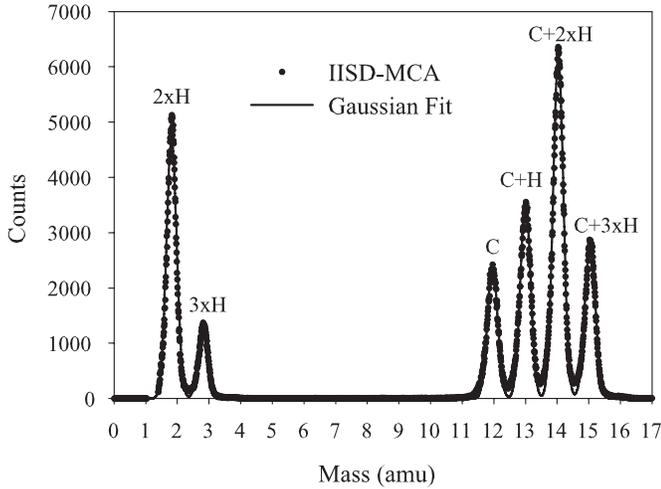
Figure 3. Background-corrected MCA data taken with the grid in.

Figure 4. Collision-energy-dependent cross sections for the DR of CH_3^+; current results and calculations reported by Douguet et al. convoluted by the electron energy spread in the electron cooler at CRYRING (Douguet et al. 2012; V. Kokoouline 2012, private communication). The energies of the four fundamental vibrational modes (in the ground electronic state) are indicated by the dashed vertical lines, as are the first two electronically excited states. The calculated uncertainties of 15% are indicated for the first few data points at low collision energies.

DR fragment spectrum at ≈ 0 eV relative collision energy shown in Figure 3 (dots) was obtained.

The relationship between the six peaks observed in the data and the contributions from each of the five open channels in Equation (1) to these peaks is described by the following linear matrix equation (Neau et al. 2000; Thomas 2008; Larsson & Orel 2008):

$$\begin{pmatrix} I_{C+3H} \\ I_{C+2H} \\ I_{C+H} \\ I_{C} \\ I_{3H} \\ I_{2H} \end{pmatrix} = \begin{pmatrix} T & T^2 & T^3 & T^2 & T^3 \\ 0 & T\bar{T} & 2T^2\bar{T} & 0 & T^2\bar{T} \\ 0 & 0 & T\bar{T}^2 & T\bar{T} & T^2\bar{T} \\ 0 & 0 & 0 & 0 & T\bar{T}^2 \\ 0 & 0 & 0 & 0 & T^2\bar{T} \\ 0 & 0 & T^2\bar{T} & T\bar{T} & T\bar{T}^2 \end{pmatrix} \begin{pmatrix} N_1 \\ N_2 \\ N_3 \\ N_4 \\ N_5 \end{pmatrix}, \quad (5)$$

where I_X corresponds to the background-corrected counts in each of the peaks in the spectra, obtained by Gaussian fits to the individual peaks, and N_1–N_5 correspond to the five energetically open product channels given in Equation (1). The branching fractions into these channels, n_1–n_5, are obtained by normalizing the solutions for N_1–N_5 as

$$n_i = \frac{N_i}{\sum_{i=1}^{5} N_i}. \quad (6)$$

The system of equations is overdetermined. To minimize any uncertainties, several different fittings were undertaken involving the full set of six peaks and five channels and also involving different combinations of five peaks with the five channels (the latter fits are not overdetermined). The known uncertainty in the transmission was also taken into consideration in each case. The final value is taken as a strict average of all of the results. The uncertainties associated with the values for the chemical branching fractions are dominated by the uncertainty in the transmission factor, T. The contribution from the statistical uncertainties associated with counting particles (I_X) are minimized by measuring for a sufficiently long period.

4. EXPERIMENTAL RESULTS

4.1. Cross Sections and Rate Coefficients

The experimentally measured DR cross sections as a function of collisional energy are shown in Figure 4. The theoretical
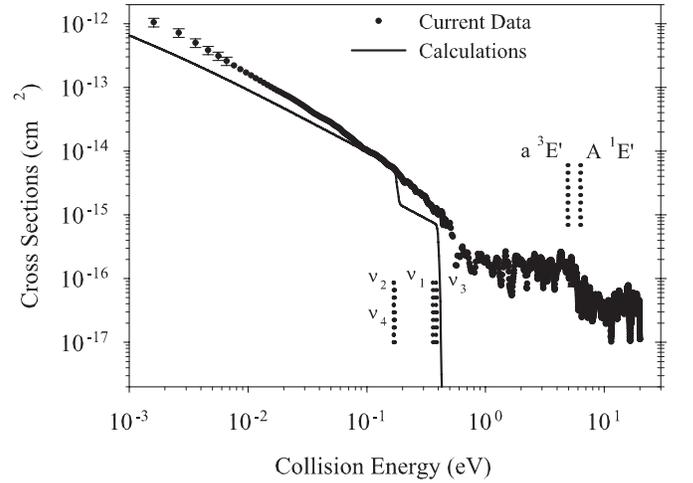
calculations for the cross sections reported by Douguet and co-workers (Douguet et al. 2012; V. Kokoouline 2012, private communication) are also plotted in Figure 4, as are the energies of the four fundamental vibrational modes (in the ground electronic state) and of the first two electronically excited states in CH_3^+: ν_1 (0.361 eV), ν_2 (0.168 eV), ν_3 (0.385 eV), ν_4 (0.170 eV), and a^3E' (4.919 eV) and A^1E' (6.258 eV), respectively. The energy for ν_1 is determined from the calculations reported by Liu et al. (2001), while all the others are calculated from data given in the NIST webbook[5].

The cross sections monotonically decrease for low collision energies until ≈ 0.1 eV where there is a break in the slope and it becomes steeper. A second break in the slope of the data is observed at ≈ 0.4 eV, and possibly a third at ≈ 0.6 eV, after which significant structures are observed in the cross sections for collision energies in the range 1–≈ 20 eV where no single slope can adequately describe the trends in these data. A best fit to the cross-section data gives the following values for the slopes describing the three indicated low collision-energy regions: $\sigma(E < 0.1 \text{ eV}) = 1.17(\pm 0.05) \times 10^{-15}E^{-1.09(\pm 0.03)}$ cm^2, $\sigma(0.1 \text{ eV} < E < 0.4 \text{ eV}) = 2.88(\pm 0.15) \times 10^{-16}E^{-1.63(\pm 0.04)}$ cm^2, and $\sigma(0.4 \text{ eV} < E < 0.6 \text{ eV}) = 1.30(\pm 0.08) \times 10^{-17}E^{-2.51(\pm 0.15)}$ cm^2 (these regions correspond to electron kinetic temperatures of $< 0.77 \times 10^3$ K, 0.77×10^3–3.10×10^3 K, and 3.10×10^3–4.60×10^3 K, respectively).

For the first region, the slope of $\approx E^{-1}$ is indicative of a process which follows the Wigner threshold behavior and breaks close to where the two lowest vibrational states in CH_3^+: $\nu_{1,4}$ lie in energy. The slope describing the experimental data up to the first break, the position of this break, as well as the value of the cross section at the break are in good agreement with the theoretical calculations (Douguet et al. 2012; V. Kokoouline 2012, private communication), where they ascribe the drop in the cross-section data to the opening of new autoionization channels from CH_3^* Rydberg states coupled to the CH_3^+: $\nu_{1,4}$ ion core.

---

[5] http://webbook.nist.gov

The drop observed in the experimental data is significantly less pronounced than that reported in the calculations, which shows a vertical step (due to the method used in the calculations). The second break in the slope occurs at ≈ 0.4 eV, close to where the next free vibrational states in CH_3^+: $\nu_{2,3}$ as well as the first vibrational combination bands, CH_3^+: ν_{2+4}, lie in energy. There is again good agreement on the position of this break with the calculations, differing again only in the steepness of the drop. The scatter in the data increases as the collision energy becomes greater than ≈ 0.5 eV, as the cross section is now more than a factor of 10^3 smaller than it is at 0.001 eV, but a third break in the slope cross section could be argued for at a collision energy of ≈ 0.6 eV, which is where the next vibrational combinational bands start to arise, e.g., ν_{1+4}.

Up to a collision energy of $\approx 6.0 \times 10^{-2}$ eV the measured data are slightly larger than the calculated values, after which point and up till the first break the values are within the experimental uncertainties and in better agreement. Similar behavior is observed between the first and second breaks: the measured data are larger than the calculations though closer in agreement at the break in the slope. The DR calculations were undertaken with a rotational temperature that was much larger than the rotational spacing (a few dozen cm^{-1}, i.e., a few dozen Kelvin/1–2 meV), but significantly smaller than the vibrational spacing (1400 cm^{-1}, 2000 K/175 meV) (V. Kokooline 2012, private communication), although rotation-dependent calculations were not undertaken. Vibrational lifetime calculations undertaken here, and discussed in the next section in detail, support the assertion that all the CH_3^+ ions stored in the ring have sufficient time (≈ 4.5 s) to radiatively decay down into the vibronic ground state before the measurement cycle is started, especially with respect to the symmetric ν_1 mode. Therefore, it is suggested that the difference between the experimental and calculated cross-section data is due to the rotational energy of the ions stored in the ring.

Highly rotationally excited ions have been observed for ions (H_3O^+, which also has D_{3h} symmetry) created in hot Penning ionization sources (Buhr et al. 2010), although reasonably efficient rotational cooling of such hot ions through interactions with the cold electrons in the interaction region has also been reported, especially for H_3^+ where detailed studies have been reported (Petrignani et al. 2011). The cold-cathode ion source used in the current experiment typically creates ions with initial rotational populations described by temperatures in the region 600–1000 K (see, e.g., measurements on N_2^+ reported by Rosen et al. 2001). CH_3^+ has a significant rotational constant of about 9.3 cm^{-1} (Jagod et al. 1994) and coupled with the storage time the ions have for interacting with the cold electrons to reduce their rotational energy, the final rotational temperature is possibly at the lower end of this temperature region, i.e., 600 K, although we cannot be certain.

At collision energies greater than 1.0 eV no single slope can describe the trend in the cross-section data due to the multiple structures observed over the region 1 to ≈ 20 eV. These structures can be related to one or all of the following effects. Indicated in Figure 4 are the first two electronically excited states in CH_3^+ (a^3E' at ≈ 4.92 eV and A^1E' at ≈ 6.26 eV), and an indirect DR mechanism via capture into Rydberg states converging to these electronically excited states is likely. The existence of other non-DR reactions, such as DE and DI are also relevant at these collision energies. DE and DI (which involve the production of a single positively charged fragment (DE) and multiple positively charged fragments (DI) with one or more neutral fragments)
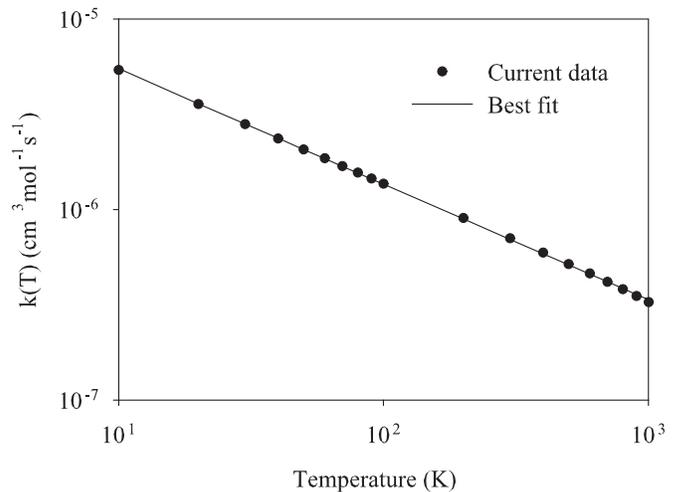

Figure 5. Derived thermal rate coefficients over the range of 10–1000 K, along with the best fit of $k(T) = 6.97 \times 10^{-7}(T/300)^{-0.61}$ cm^3 s^{-1}.

become energetically accessible at ≈ 5.5 eV (DE; $CH_2^+ + H$, $CH^+ + H_2$) and ≈ 21 eV (DI; $CH_2^+ + H^+$), respectively. Although both DI and DE are competing reaction mechanisms to DR, i.e., they remove flux from the DR reaction, they (importantly) indicate an increase in the density of highly excited neutral states into which the electron can be captured in the DR process, thus increasing the possibility that the DR process will continue to completion. Both the DE and DI of CH_3^+ have been measured (in which the heavy ion-fragments are detected; C_n^+; Bahati et al. 2009) and these data are consistent with a threshold for the lowest DE channels of ≈ 5.0 eV. The relatively flat behavior of the cross-section data for the DR reactions over the region 1–5 eV could therefore be related to the indirect mechanism via the Rydberg states converging to the electronically excited ion cores while the immediate decrease in the general slope of the cross-section data over the region 5–10 eV, with a local minima at ≈ 10 eV, could indicate that the DE reaction successfully removes flux from the DR reaction channel. In their DE measurements, Bahati et al. (2009) report that the DE reaction plateaus between 10 and 20 eV, i.e., before the DI reaction opens up, and that over the same energy region in the DR data reported here, the DR cross sections significantly increase and subsequently plateau. Bahati et al. (2009) report a value from all heavy-ion contributions to the DE cross sections in this plateau region of $\approx 1.23 \times 10^{-16}$ cm^{-2}, which is approximately the same as that observed here for the DR reaction.

The general form of the cross-section data reported here is in good agreement between 0.1 and 10 eV with the data reported by Vejby-Christensen et al. (1997). At low collision energies the data diverge, though this is generally explained by the difference in the transverse electron energy in the two storage rings (1–2 meV at CRYRING and 22 meV at ASTRID) and has been consistently observed in other DR measurements carried out at the two storage rings (Al-Khalili et al. 2003).

The calculated thermal rate coefficients are displayed in Figure 5, along with the best fit over the temperature range of 10–1000 K. Our result, $k(T) = 6.97(\pm 0.03) \times 10^{-7}(T/300)^{-0.61(\pm 0.02)}$ cm^3 s^{-1}, is not entirely dissimilar from the value of $k(T) = 8.0 \times 10^{-7}(T/300)^{-0.53}$ cm^3 s^{-1} reported from the single-pass merged-beam experiment (Sheehan & St.-Maurice 2004), with the differences most likely due to the influence of vibrational excitation in the earlier experiment.

Table 1
The Chemical Branching Fractions Determined
for the DR of CH_3^+ with ≈ 0 eV Electrons

Channel	Present Data	(Vejby-Christensen et al. 1997)
CH_3	$0.00^{+0.01}_{-0.00}$	N/A
$CH_2 + H$	$0.35^{+0.01}_{-0.01}$	$0.40^{+0.10}_{-0.10}$
$CH + 2H$	$0.20^{+0.02}_{-0.02}$	$0.16^{+0.15}_{-0.15}$
$CH + H_2$	$0.10^{+0.01}_{-0.01}$	$0.14^{+0.10}_{-0.10}$
$C + H_2 + H$	$0.35^{+0.01}_{-0.02}$	$0.30^{+0.08}_{-0.08}$

Table 2
Fundamental Frequencies and Einstein Coefficients for Spontaneous Emission
Calculated by the VCI Method, along with Experimental Values

Mode	Frequency (cm^{-1})		A (s^{-1})	
	VCI	Expt.	$\nu_1 \rightarrow \nu_n$[a]	$\nu_n \rightarrow 0$[b]
$\nu_1(A_1)$	2939.8	...	...	0.01
$\nu_2(A_2)$	1382.7	1359 ± 7[c]	0.63	2.65
$\nu_3(E')$	3085.3	3108.38[c]	...	89.02
$\nu_4(E')$	1384.2	1370 ± 7[c]	0.89	4.43

Notes.
[a] Spontaneous emission from ν_1.
[b] Spontaneous emission to the ground state.
[c] Liu et al. (2001), Crofton et al. (1988), and http://webbook.nist.gov.

4.2. Branching Fractions

Figure 3 (solid line) plots the sum of the Gaussian best fits to the experimentally obtained pure-DR fragment energy spectra. The peak areas for each peak were determined from these fits and a least-squares approach in Matlab was used to solve Equation (5). Table 1 lists the experimentally measured chemical branching fractions in the DR of CH_3^+ with ≈ 0 eV electrons obtained from the current study along with those reported by Vejby-Christensen et al. (1997).

Within the quoted uncertainties, especially with the large uncertainties of Vejby-Christensen et al. (1997), the branching fraction data are in good agreement. It is worth commenting that the previously reported tendency for small polyatomic molecular ions to undergo quite destructive fragmentation in low-energy DR reactions, i.e., multiple bond breaking (Thomas 2008), is also observed here and represents 65% of the observed reaction flux ($CH + 2H$, $CH + H_2$, and $C + H_2 + H$). This is in stark contrast to the $\sim$90% CH_2 production assumed in the astrochemical models of van Dishoeck & Black (1989).

The formation of H_2 occurs in 45% of all reactions, and this process requires a significant degree of geometrical rearrangement in the reaction process. The production of molecular hydrogen from the DR of similar, small polyatomic molecular ions has also been reported (Thomas 2008), and this is attributed to the significant mobility of the hydrogen atoms/protons in these systems, most likely mediated by bending vibrations in super-bent electronic states (Thomas 2008).

5. VIBRATIONAL CALCULATIONS

When CH_3^+ ions are produced in the ion source, they are produced in a variety of vibrational states. All states that are connected to lower states by infrared-active transitions will be drained of all population via spontaneous emission on timescales shorter than a second. However, the $\nu_1(A_1)$ mode is infrared-inactive, and to our knowledge there have been no calculations or experiments to determine the rate of spontaneous emission from ν_1 to lower states. As the DR rate of molecular ions can depend sensitively on the vibrational state, see, e.g., Zhaunerchyk et al. (2007, H_2^+) and Petrignani et al. (2005, O_2^+), it is critical to estimate this spontaneous emission rate. If it is fast enough, then all of the CH_3^+ ions in the ring will relax to the vibrational ground state before the DR measurements begin, and the resulting thermal rate coefficients will be appropriate for modeling the interstellar medium (where collision/reaction timescales are long enough to ensure vibrational relaxation before recombination).

To estimate the spontaneous emission rate of CH_3^+ from the $\nu_1(A_1)$ state to the $\nu_2(A_2)$ and $\nu_4(E')$ states, we have carried out vibrational calculations using the potential energy surface (PES) and the dipole moment surface (DMS) derived from ab initio

electronic structure theory. We employed the PES developed by Keçeli et al. (2009), which was determined by coupled cluster theory at the highly accurate complete basis set limit (Hirata et al. 2004). The PES is expanded in terms of normal coordinate couplings (Carter et al. 1997) and truncated at the third order,

$$V(\mathbf{Q}) = V_0 + \sum_i V_i(Q_i) + \sum_{i<j} V_{ij}(Q_i, Q_j)$$
$$+ \sum_{i<j<k} V_{ijk}(Q_i, Q_j, Q_k), \quad (7)$$

where Q_i denotes the ith normal coordinate. The DMS has been newly constructed up to three-mode coupling at the MP2/aug-cc-pVTZ level of theory (Møller & Plesset 1934; Kendall et al. 1992). The vibrational wave functions have been obtained by the vibrational configuration interaction (VCI) method based on the vibrational self-consistent field (VSCF; Bowman et al. 2003; Yagi et al. 2000; Hirata & Yagi 2008). For more details, see Keçeli et al. (2009).

The Einstein coefficient for spontaneous emission has been calculated by the following formula (in atomic units):

$$A = \frac{4}{3}\left(\frac{\omega_{fi}}{c}\right)^3 |\mu_{fi}|^2, \quad (8)$$

where c denotes the speed of light, and ω_{fi} and μ_{fi} are the transition frequency and transition dipole moment, respectively. As a preliminary check, we have applied the method to H_3^+ (with a PES/DMS generated at the MP2/aug-cc-pVTZ level) and confirmed that the present calculation agrees reasonably well with the previous calculation: 153.0 (128.8) and 0.54 (0.85) s^{-1} (numbers in parentheses are from Dinelli et al. 1992) for the $\nu_2 \rightarrow 0$ and $\nu_1 \rightarrow \nu_2$ transitions, respectively. All the electronic and vibrational structure calculations were performed by the Gaussian09 (Frisch et al. 2010) and SINDO[6] (Yagi 2011) programs, respectively.

The calculated Einstein A coefficients are listed in Table 2 together with the vibrational energy levels and available experimental values. It is found that the rates of spontaneous emission are 0.63 and 0.89 s^{-1} for the $\nu_1 \rightarrow \nu_2$ and $\nu_1 \rightarrow \nu_4$ transitions, respectively, and that further emissions to the ground state are much faster. The calculated wave function of ν_1 is found to be mixed with those of $2\nu_2$ and $2\nu_4$ by 8.4% and 6.5%. These components, though a small fraction, essentially determine the rate of emission, since the $2\nu_2 \rightarrow \nu_2$ and $2\nu_4 \rightarrow \nu_4$ transitions,

---

[6] SINDO is a suite of programs including a PES/DMS generator and solver of the vibrational many-body problem developed at the University of Tokyo.
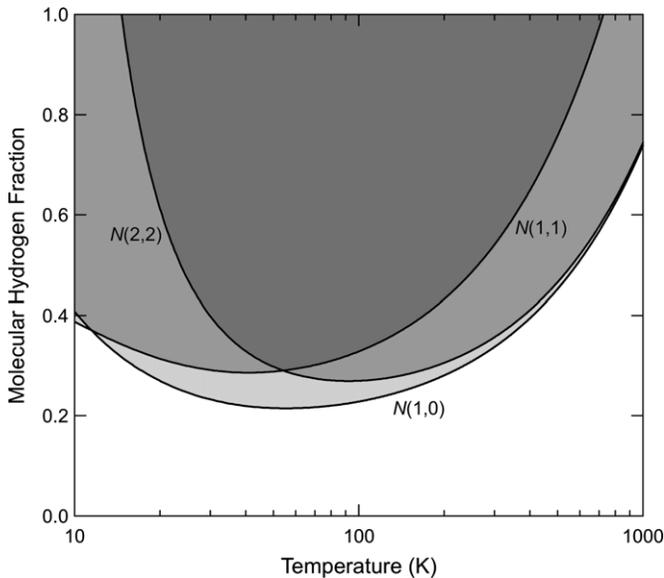
Figure 6. Plot of the (f,T) parameter space for the sightline toward Cygnus OB2 12. The three solid curves represent contours corresponding to the values of f and T which reproduce the ratios $N(1,0)/N(CH^+)$, $N(1,1)/N(CH^+)$, and $N(2,2)/N(CH^+)$ (where the $N(J,K)$ values are 3σ upper limits) defined via Equation (8) in Indriolo et al. (2010) and $N(CH^+)$ is the observed CH^+ column density. The shaded regions are excluded by our analysis, and progressively darker shading indicates regions excluded by more than one transition.

which are allowed by the linear term of the DMS, make the dominant contributions to the transition dipole moments of the "forbidden" transitions $\nu_1 \rightarrow \nu_2$ and $\nu_1 \rightarrow \nu_4$. This intensity borrowing is the mechanism of the relatively fast decay of ν_1.

Our results indicate that the vibrationally hot CH_3^+ molecules produced by the ion source decay reasonably fast to the vibrational ground state while they are stored in the ring, similar to the case of H_3^+ (Kreckel et al. 2002).

6. ASTROPHYSICAL IMPLICATIONS

The CH^+ ion is ubiquitously observed in sightlines containing diffuse interstellar clouds; in fact, it was one of the first interstellar molecules to be identified. However, the large observed abundance of CH^+ remains somewhat enigmatic, as CH^+ is destroyed quickly by reactions with H, H_2, and electrons, but there is no known efficient exothermic formation mechanism. Consequently, additional observational constraints on the nature of the gas where CH^+ exists would be very helpful.

Indriolo et al. (2010) suggested that infrared observations of CH_3^+ could provide useful information about the CH^+-bearing gas. In an environment where H_2 is present, it will react with CH^+ at the Langevin rate to produce CH_2^+, which in turn can react with H_2 to form CH_3^+. However, CH_3^+ does not react with H_2 (except very slowly by radiative association to form CH_5^+), since the hydrogen abstraction reaction to form CH_4^+ is endothermic. The relative abundance of CH_3^+ to CH^+ therefore depends on the molecular hydrogen fraction ($f \equiv 2n(H_2)/(n(H)+2n(H_2))$) and also on the electron temperature (through the DR rate).

Indriolo et al. (2010) performed a sensitive search for three transitions [$^r R(1,0)$, $^r R(1,1)$, and $^r R(2,2)$] arising from the lowest rotational levels of CH_3^+ in the diffuse cloud sightline toward Cygnus OB2 12, but did not detect it. These data were used to determine an upper limit to the column density for each of the three states, $N(J, K)$, and the resulting upper limits on the $N(J, K)/N(CH^+)$ ratio were used to exclude certain regions of

the (f, T) parameter space. However, their analysis depended on earlier DR measurements, which for the vibrational ground state were taken to be uncertain to a factor of three in either direction. As a result, the excluded regions were highly uncertain: at 100 K, the excluded molecular fraction was either $f \gtrsim 0.25$ or $f \gtrsim 0.07$, depending on the actual DR rate. At 1000 K, either $f \gtrsim 0.18$ was excluded, or there was no constraint at all on the molecular fraction, again depending on the correct DR rate.

The present measurements on the ground vibrational state of CH_3^+, in which absolute values for the temperature-dependent rate coefficient are determined, now allow a more rigorous determination of the excluded region, as shown in Figure 6. Molecular fractions less than 0.2 are no longer excluded at any temperature, and for high temperatures of $\sim$1000 K only the highest molecular fractions ($f \gtrsim 0.75$) can be excluded. Future observations with higher sensitivity can be expected to either lower the excluded regions in this parameter space (in the event of a tighter upper limit), or to provide a narrow allowed region of parameter space (in the case of a detection).

7. CONCLUSION

The DR reaction of vibrationally cold CH_3^+ ions with low-energy electrons was measured at the heavy ion storage ring CRYRING. The reaction at $\approx$0 eV collision energy is dominated by the fracture of multiple C–H bonds, with 65% of the reaction flux producing $CH + 2H$, $CH + H_2$, and $C + H_2 + H$. Uncertainties in the chemical branching fractions have been reduced by almost an order of magnitude compared to previous storage ring measurements (Vejby-Christensen et al. 1997). Several features are observed in the energy-dependent reaction cross section. At collision energies relevant to the interstellar medium, the cross section monotonically decreases until about $\approx$0.1 eV where there is a break in the slope and it becomes steeper. A second break in the slope of the data is observed at about $\approx$0.4 eV, and possibly another at $\approx$0.6 eV, after which significant structures are observed in the cross section for collision energies in the range 1–$\approx$20 eV and no slopes can describe the trends in the data. The thermal rate coefficient has been derived to be $k(T) = 6.97 \times 10^{-7}(T/300)^{-0.61}$ cm^3 s^{-1} over the region 10 K $\leqslant$ $T \leqslant$ 1000 K. Vibrational calculations confirm that vibrationally excited CH_3^+ can relax to the ground state by spontaneous emission in $\sim$1 s, considerably shorter than the storage time in the ring. As one important example of an astrophysical application, our DR rate coefficient for vibrationally cold CH_3^+ can now enable more meaningful constraints on the hydrogen molecular fraction and the temperature in the regions of the diffuse interstellar medium where CH^+ is abundant.

REFERENCES

Al-Khalili, A., Rosén, S., Danared, H., et al. 2003, Phys. Rev. A, 68, 042702
Bahati, E. M., Fogle, M., Vane, C. R., et al. 2009, Phys. Rev. A, 79, 052703
Balsiger, H., Altwegg, K., Buhler, F., et al. 1987, A&A, 187, 163
Bardsley, J. N. 1968, J. Phys. B: At. Mol. Phys., 1, 365
Bates, D. R. 1950, Phys. Rev., 77, 718
Bowman, J. M., Carter, S., & Huang, X. C. 2003, Int. Rev. Phys. Chem., 22, 533
Buhr, H., Stützel, J., Mendes, M. B., et al. 2010, Phys. Rev. Lett., 105, 103202
Carter, S., Culik, S. J., & Bowman, J. M. 1997, J. Chem. Phys., 107, 10458
Crofton, M. W., Jagod, M.-F., Rehfuss, B. D., Kreiner, W. A., & Oka, T. 1988, J. Chem. Phys., 88, 666

Danared, H., Andler, G., Bagge, L., et al. 1994, Phys. Rev. Lett., 72, 3775
Danared, H., Källberg, A., Andler, G., et al. 2000, Nucl. Instrum. Methods Phys. Res. A, 441, 123
DeWitt, D. R., Schuch, R., Gao, H., et al. 1996, Phys. Rev. A, 53, 2327
Dinelli, B. M., Miller, S., & Tennyson, J. 1992, J. Mol. Spectrosc., 153, 718
Douguet, N., Orel, A. E., Greene, C. H., & Kokoouline, V. 2012, Phys. Rev. Lett., 108, 023202
Frisch, M. J., Trucks, G. W., Schlegel, H. B., et al. 2010, Gaussian09 (Revision B.01; Wallingford, CT: Gaussian Inc.)
Haider, S., Bhardwaj, A., & Singhal, R. 1993, Icarus, 101, 234
Hirata, S., Fan, P.-D., Auer, A. A., Nooijen, M., & Piecuch, P. 2004, J. Chem. Phys., 121, 12197
Hirata, S., & Yagi, K. 2008, Chem. Phys. Lett., 464, 123
Hollis, J. M., Jewell, P. R., & Lovas, F. J. 1995, ApJ, 438, 259
Indriolo, N., Oka, T., Geballe, T. R., & McCall, B. J. 2010, ApJ, 711, 1338
Jagod, M.-F., Gabrys, C. M., Rösslein, M., Uy, D., & Oka, T. 1994, Can. J. Phys., 72, 1192
Keçeli, M., Shiozaki, T., Yagi, K., & Hirata, S. 2009, Mol. Phys., 107, 1283
Kendall, R. A., Dunning, T. H., Jr., & Harrison, R. J. 1992, J. Chem. Phys., 96, 6796
Kim, Y., & Fox, J. 1994, Icarus, 112, 310
Kreckel, H., Krohn, S., Lammich, L., et al. 2002, Phys. Rev. A, 66, 052509
Lampert, A., Wolf, A., Habs, D., et al. 1996, Phys. Rev. A, 53, 1413
Larsson, M., & Orel, A. E. 2008, Dissociative Recombination of Molecular Ions (Cambridge: Cambridge Univ. Press)
Liu, X., Gross, R. L., & Suits, A. G. 2001, Science, 294, 2527
Møller, C., & Plesset, M. S. 1934, Phys. Rev., 46, 618

Mowat, J. R., Danared, H., Sundström, G., et al. 1995, Phys. Rev. Lett., 74, 50
Mul, P. M., Mitchell, J. B. A., D'Angelo, V. S., et al. 1981, J. Phys. B: At. Mol. Phys., 14, 1353
Neau, A., Al Khalili, A., Rosén, S., et al. 2000, J. Chem. Phys., 113, 1762
Paal, A., Simonsson, A., Dietrich, J., & Mohos, I. 2006, in Proc. EPAC 2006 (Mulhouse: European Physical Society Accelerator Group), 1196
Peterson, J. R., Padellec, A. L., Danared, H., et al. 1998, J. Chem. Phys., 108, 1978
Petrignani, A., Altevogt, S., Berg, M. H., et al. 2011, Phys. Rev. A, 83, 032711
Petrignani, A., van der Zande, W. J., Cosby, P. C., et al. 2005, J. Chem. Phys., 122, 014302
Rosen, S., Larsson, M., Royen, P., et al. 2001, Rev. Sci. Instrum., 72, 4300
Rubin, M., Hansen, K. C., Gombosi, T. I., et al. 2009, Icarus, 199, 505
Salonen, E., Nordlund, K., Keinonen, J., & Wu, C. 2002, Contrib. Plasma Phys., 42, 458
Sheehan, C., & St.-Maurice, J.-P. 2004, Adv. Space Res., 33, 216
Smith, D. 1992, Chem. Rev., 92, 1473
Thomas, R. D. 2008, Mass Spectrom. Rev., 27, 485
van Dishoeck, E. F., & Black, J. H. 1989, ApJ, 340, 273
Vejby-Christensen, L., Andersen, L. H., Heber, O., et al. 1997, ApJ, 483, 531
Westlake, J. H., Waite, J. H., Jr., Mandt, K. E., et al. 2012, J. Geophys. Res., 117, E01003
Wigner, E. P. 1948, Phys. Rev., 73, 1002
Yagi, K. 2011, SINDO (Tokyo: Univ. Tokyo)
Yagi, K., Taketsugu, T., Hirao, K., & Gordon, M. S. 2000, J. Chem. Phys., 113, 1005
Zhaunerchyk, V., Al-Khalili, A., Thomas, R. D., et al. 2007, Phys. Rev. Lett., 99, 013201